


Effects of chemical defects on anisotropic dielectric response of polyethylene

Cite as: AIP Advances 9, 045022 (2019); <https://doi.org/10.1063/1.5093566>

Submitted: 22 February 2019 . Accepted: 08 April 2019 . Published Online: 19 April 2019

Shogo Fukushima, Subodh Tiwari, Hiroyuki Kumazoe, Rajiv K. Kalia, Aiichiro Nakano , Fuyuki Shimojo, and Priya Vashishta



View Online



Export Citation



CrossMark

AVS Quantum Science

Co-published with AIP Publishing



Coming Soon!

Effects of chemical defects on anisotropic dielectric response of polyethylene

Cite as: AIP Advances 9, 045022 (2019); doi: 10.1063/1.5093566

Submitted: 22 February 2019 • Accepted: 8 April 2019 •

Published Online: 19 April 2019



View Online



Export Citation



CrossMark

Shogo Fukushima,¹ Subodh Tiwari,² Hiroyuki Kumazoe,¹ Rajiv K. Kalia,² Aiichiro Nakano,^{2,a)}  Fuyuki Shimojo,¹ and Priya Vashishta²

AFFILIATIONS

¹Department of Physics, Kumamoto University, Kumamoto 860-8555, Japan

²Collaboratory for Advanced Computing and Simulations, Department of Physics & Astronomy, Department of Computer Science, Department of Chemical Engineering & Materials Science, University of Southern California, Los Angeles, California 90089-0242, USA

^{a)}anakano@usc.edu

ABSTRACT

Dielectric polymers such as polyethylene (PE) have a wide range of energy and electronic applications. While recent studies have shown significant effects of chemical defects on the electronic structure of PE, those on the dielectric properties remain elusive. Here, first-principles quantum-mechanical calculations show anisotropic dielectric constants of PE, which are sensitive to the type of defects. Specifically, addition of iodine defects increases the high-frequency dielectric constant. Addition of hydroxyl or carboxyl group, on the other hand, causes noticeable anisotropic changes in the static dielectric constant, which is well elucidated through the rotation and concerted motions of chemical groups. The sensitivity of these defects may be exploited to rationally alter the behavior of PE.

© 2019 Author(s). All article content, except where otherwise noted, is licensed under a Creative Commons Attribution (CC BY) license (<http://creativecommons.org/licenses/by/4.0/>). <https://doi.org/10.1063/1.5093566>

Dielectric materials have a wide range of applications ranging from capacitors, field-transistors and high-voltage cables to transistors.¹⁻⁵ Both inorganic and organic materials have been used as dielectric materials. Inorganic materials show exceptionally large dielectric constants but suffer from low breakdown strength. Organic polymers, on the other hand, have low dielectric constants but extremely high breakdown potential. For high-voltage applications, organic polymers are thus generally preferred over inorganic dielectrics.⁶ An archetypal dielectric polymer is polyethylene (PE),⁷ which is primarily used due to cost effectiveness, low weight, ease of processing and high resistivity and high breakdown strength.^{8,9-10}

PE has unusual electronic structures such as negative electron affinity in its crystalline form.¹¹ Also, various processing methods for PE introduce defects such as amorphous region, polymer chain bending, chain end and chemical defects.⁵ Recent studies have shown important effects of chemical⁸ and morphological¹² defects on the electronic structures (*e.g.*, energy levels of electron and hole trap states) of PE.¹³ These defects may also play crucial roles in determining dielectric properties of PE crystal. Thus, understanding

the change in local geometries due to chemical defects and effects of these changes on dielectric properties under high electric field is extremely important.

Despite their importance, effects of chemical defects on the dielectric response of PE remains elusive. In this paper, we use first-principles quantum-mechanical calculations to show that PE exhibits highly anisotropic dielectric response that depends sensitively on the type of chemical defects.

Quantum-mechanical calculations in the framework of density functional theory (DFT) have successfully been used for determining various material properties.¹⁴⁻¹⁷ To study dielectric properties of solids, in particular, several methods have been proposed, which introduce finite electric field in the presence of periodic boundary conditions.¹⁸⁻²⁰ Here, we follow the work of Umari *et al.* for the treatment of homogeneous electric field within first principles calculations.¹⁸ This method has been implemented in our own software package.²¹ Energy of a metastable state induced by finite electric field within periodic boundary condition is given by

$$E^E[\{\psi_i\}] = E^0[\{\psi_i\}] - \Omega E \cdot P[\{\psi_i\}], \quad (1)$$

where $E^0[\{\psi_i\}]$ is the ground-state energy functional, $P[\{\psi_i\}]$ is the polarization along the direction of electric field E and Ω is the volume of the adopted cell. Polarization is defined by Resta.²²

$$P[\{\psi_i\}] = -\frac{L}{\pi} \text{Im} \left(\ln \det \left[\left\langle \psi_i \left| e^{\frac{2\pi i}{L} \cdot} \right| \psi_i \right\rangle \right] \right). \quad (2)$$

The high-frequency dielectric constant ϵ_∞ within the linear-response regime is estimated as

$$\epsilon_\infty = 1 + 4\pi \frac{\Delta P^E}{E}, \quad (3)$$

where ΔP^E is the change in polarization due to finite electric field for fixed atomic positions and E is the applied electric field. Next, change in polarization due to atomic relaxation is obtained by performing damped molecular dynamics. Static dielectric constant is then computed from the high-frequency dielectric constant and change in polarization constant due to atomic relaxation as

$$\epsilon_0 = \epsilon_\infty + \Delta\epsilon. \quad (4)$$

Detailed description of simulation methods is provided in [supplementary material](#).

The initial system (Fig. 1a) is composed of $2 \times 3 \times 4$ PE crystalline unit cells in an orthorhombic simulation box of size $14.8 \times 14.8 \times 10.136 \text{ \AA}^3$.²³ To introduce chemical defects, we replace hydrogen atom with either iodine (I), hydroxyl group (OH) or carboxyl group (COOH). We refer the systems with iodine, hydroxyl and carboxyl defects as PE-I, PE-OH and PE-COOH, respectively. These defects are specifically chosen since they frequently occur in polymer systems and are representative of physical and chemical effects arising from defects. Namely, iodine captures the effect of chemical point defects, whereas OH and COOH groups capture the essence of defect generated by chemical species with varying levels of steric effect. Figure 1, b-d, shows the studied defected systems. Defects introduced in the system are indicated by dashed ellipses in Fig. 1, b-d. Figure 1e shows a schematic of the simulation, where we applied electric field on PE along the [001] crystallographic direction.

To understand the effects of defects on anisotropic dielectric response, we compare high-frequency and static dielectric constants for all four systems (*i.e.*, PE, PE-I, PE-COOH and PE-OH), where the dielectric constants are computed for three crystallographic directions: [100], [010] and [001]. The dielectric constants are computed in the linear-response regime, where the energy functional is stable and Eq. (3) is applicable. Figure S1 in the [supplementary material](#) shows the change in polarization as a function of electric field. Polarization is a linear function of electric field in the linear-response regime for all three crystallographic directions in each system. A typical range of electric field is between 10^{-4} and 10^{-2} a.u.

Figure 2, a-c, compares the high-frequency dielectric constant (dashed lines) and static dielectric constant (solid lines) of all four systems, respectively, along [100], [010] and [001] directions. Direction-averaged static dielectric constant of PE is 2.418, which is in good agreement with an experimental value.²⁴ Figure 2d shows the difference between static and high-frequency dielectric constants ($\Delta\epsilon$) for all three directions. Note that $\Delta\epsilon$ originates from atomic relaxation in the system.¹⁸ Crystalline PE shows atomic relaxation

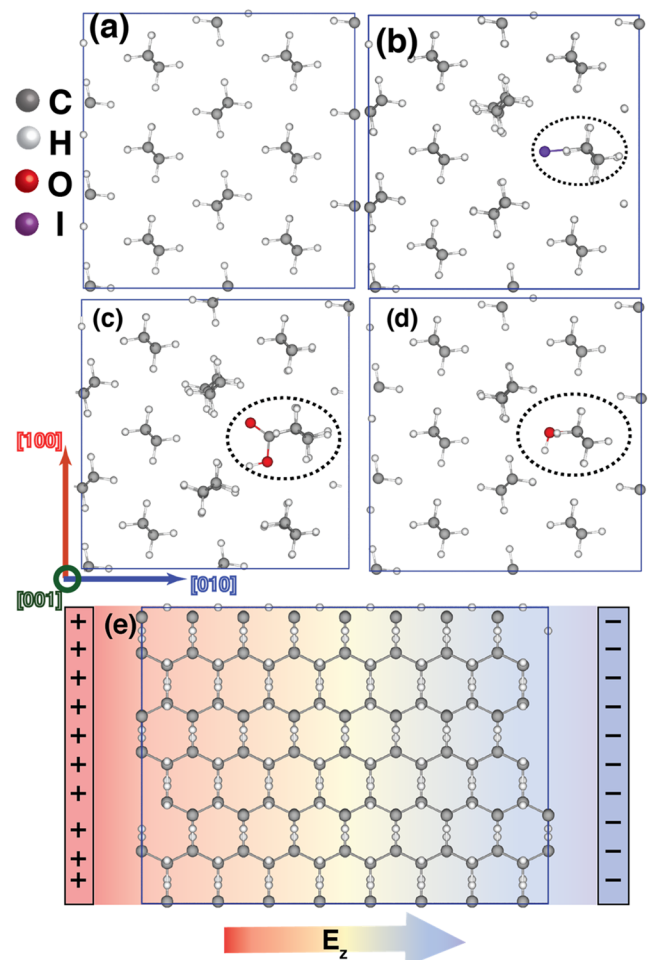


FIG. 1. Polyethylene (PE) and defected PE systems: (a) perfect PE crystal; (b) PE with iodine defect (PE-I); (c) PE with COOH defect (PE-COOH); and (d) PE with OH defect (PE-OH). The grey, white, red and purple spheres are C, H, O and I atoms, respectively. Dashed ellipses indicate defect positions. (e) Schematic of applied electric field on PE system. Color gradient and arrow represent the direction of electric field.

in [100] and [010] directions under electric field, leading to positive $\Delta\epsilon$. In [001] direction, we observe extremely small $\Delta\epsilon$, suggesting negligible atomic relaxation. This observation can be understood as a consequence of the anisotropic bonding in PE. In [100] and [010] directions, PE is only bonded with weak van der Waals (vdW) interaction. The weak vdW interaction can easily be overcome with electric field, leading to massive atomic relaxation, hence large $\Delta\epsilon$. In [001] direction, on the other hand, PE is bonded by extremely rigid covalent bonds, which largely restricts atomic relaxations, hence negligible $\Delta\epsilon$.

In Fig. 2, PE with iodine defects (PE-I) exhibits larger high-frequency dielectric constant in comparison to pure crystalline PE in all three crystallographic directions. The large ϵ_∞ associated with iodine defect can be attributed to the high polarizability of iodine. On the other hand, $\Delta\epsilon$ of PE-I is almost identical to that of crystalline

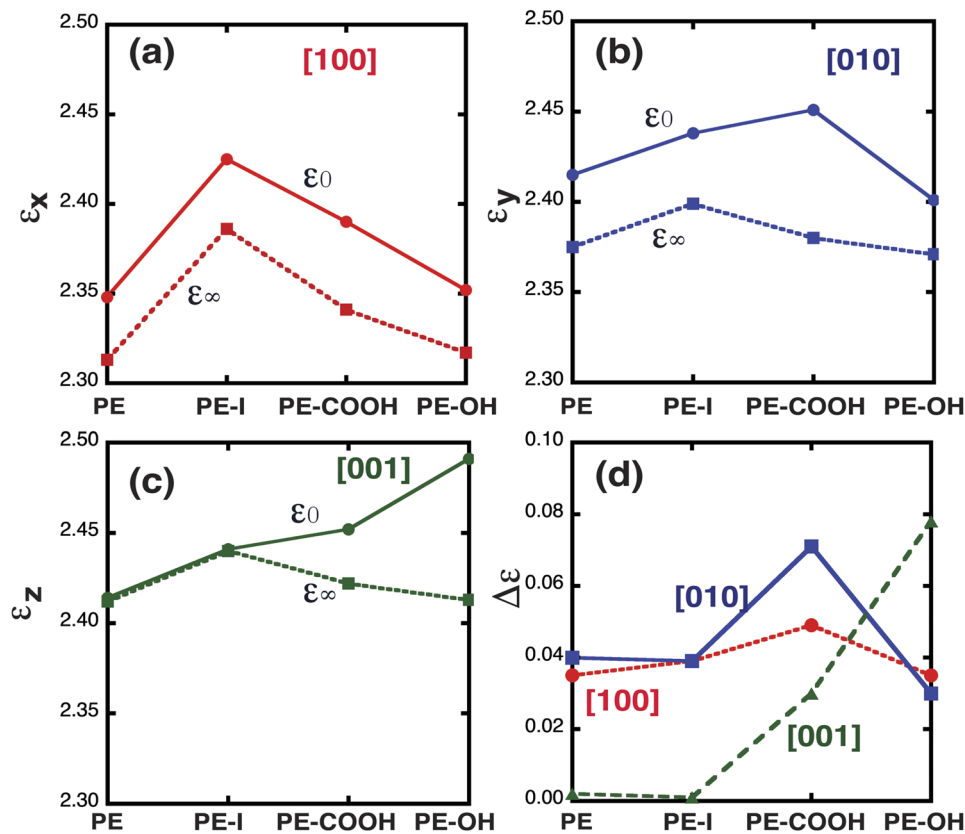


FIG. 2. Directional dependence of high-frequency (ϵ_∞) and static (ϵ_0) dielectric constants in PE crystal without and with defects. (a), (b) and (c) correspond to an applied electric field along [100], [010] and [001] directions, respectively. (d) Difference between static and high-frequency dielectric constants ($\Delta\epsilon$) along [100] (red), [010] (blue) and [001] (green) directions.

PE as shown in Fig. 2d. Namely, iodine merely acts a chemical point defect and does not offer any mean of atomic relaxation.

Introduction of carboxyl (COOH) or hydroxyl (OH) group as a chemical defect increases high-frequency dielectric constant to only some extent due to the introduction of slightly more polarizable chemical defect as shown in Fig. 2, a-c. In contrast, we observe extremely anisotropic $\Delta\epsilon$ due to their relaxations. For [001] direction, we observe an appreciable change in $\Delta\epsilon$ for PE-COOH and PE-OH systems unlike PE and PE-I as shown in Fig. 2d (green curve). This increase suggests the presence of atomic relaxation mechanisms. In [001] direction, presence of rigid covalent bonds hinders any atomic relaxation in case of PE and PE-I systems. Introduction of COOH and OH defects introduces new atomic degrees of freedom. Under electric field in [001] direction, atomic relaxation in PE backbone is not observed. However, we observe atomic relaxation in defects introduced in system. Figures 3a and 3b show relaxation of OH and COOH defects, respectively, under electric field in [001] direction. We observe rotation of H atom around C-O bond. video S3.mov shows the complete rotation after turning on the electric field of 10^{-2} a.u. In PE-COOH, we also observe similar rotation of COOH group along C-C bond. video S4.mov shows rotation of COOH defect under electric field. Since we do not observe any noticeable change in the backbone structure, the degree of rotation in defects species is proportional to the electric field applied. Figure S2 shows the energy required for rotating defect species as a function of electric field. Rotation of OH from

0° to 90° has an energy barrier of 1.84 kcal/mol. This barrier is easily overcome by applied electric field. In contrast, COOH rotation barrier is much higher (34.5 kcal/mol). Accordingly, degree of rotation of COOH is much lower compared to OH defects, leading to a lower $\Delta\epsilon$.

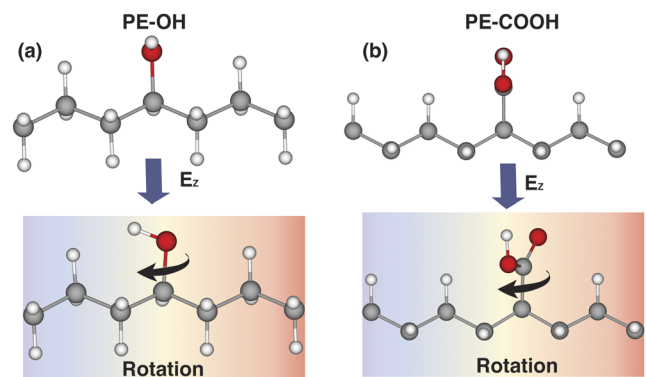


FIG. 3. Structural change in under electric field in PE with OH and COOH defects. (a) Optimized PE-OH structure in the absence of electric field (top) and final structure after optimization under an electric field of 10^{-2} a.u. in [001] direction (bottom). (b) The same for PE-COOH. Color gradient from red to blue indicates the electric-field direction.

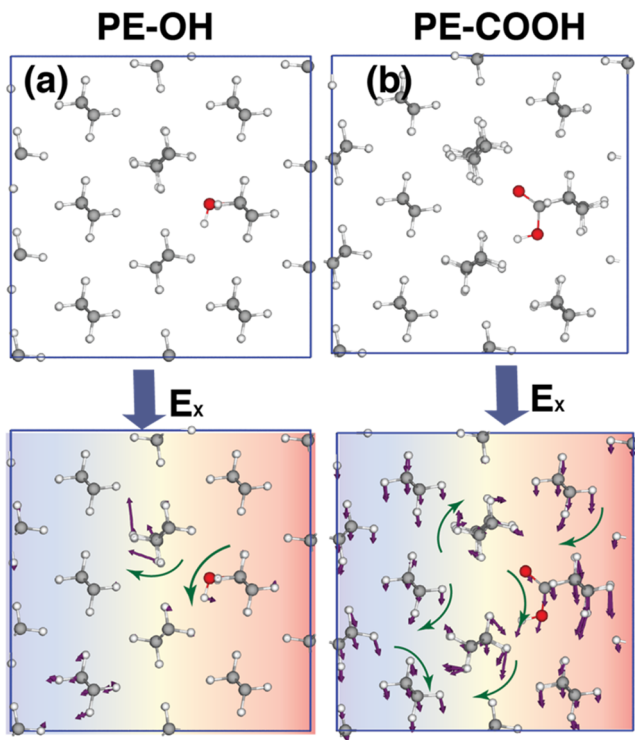


FIG. 4. Structural change in PE with OH and COOH defects under electric field. (a) Optimized structure without electric field (top) and final structure of PE with OH defect under an electric field of 10^{-2} a.u. in [100] direction. (b) The same for PE-COOH. Motion of chemical groups due to electric field is shown by arrows. Color gradient from red to blue indicates the electric field direction.

In [100] direction, $\Delta\epsilon$ has similar values for PE, PE-I and PE-OH as shown in Fig. 2d. For PE-COOH system, in contrast, we observe a larger $\Delta\epsilon \sim 0.05$ compared to all other systems. This can be attributed to steric size and the presence of polar group in PE-COOH. Figure 4, a and b, compares the atomic relaxation in PE-OH and PE-COOH, respectively, under electric field. Extremely small atomic relaxation is observed in case of OH defect. On the other hand, we observe discernable atomic relaxation for COOH group. PE-COOH system shows tilting of COOH group, along with the whole chain with which the COOH defect is attached, as shown by green arrows in Fig. 4b. This motion in turn triggers readjustment of nearby polymer chains. video S5.mov shows atomic relaxation of COOH and triggering of surrounding polymer-chain realignment. Figure 4a shows the readjustment of polymer chain due to OH group. For PE-OH system, we observe slight change in C-O-H angle, triggering minimal realignment of nearby polymer chains. Such readjustment is not observed in PE and PE-I.

In [010] direction, we also observe similar behavior as [010] direction. Figure 5, a and b, shows the relaxation mechanism for PE-OH and PE-COOH systems, respectively. Atomic relaxation mechanism for PE, PE-I and PE-OH systems are almost similar as that in [100] direction. Thus, $\Delta\epsilon$ is similar for [010] and [100] directions. However, the pronounced reordering for PE-COOH system is observed in [010], as opposed to [100] direction, leading to the

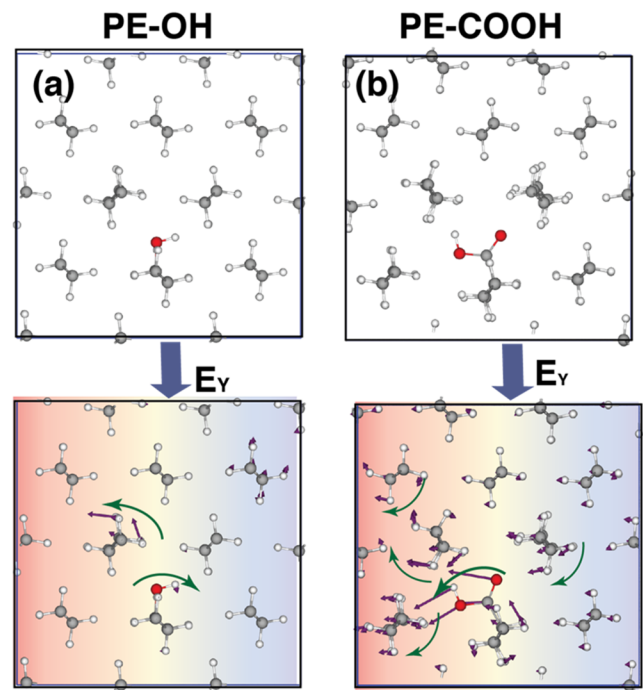


FIG. 5. Structural change in PE with OH and COOH defects under electric field. (a) Optimized structure without electric field (top) and final structure of PE with OH defect under electric field of 10^{-2} a.u. in [010] direction (bottom) in PE-OH system. (b) The same for PE-COOH system. Motion of chemical groups due to electric field is shown by arrows. Color gradient from red to blue shows the electric-field direction.

large static dielectric constant for PE-COOH system in [010] direction. This may be due to the alignment of COOH group with [010] direction.

In addition to the above-mentioned defects, we have also studied the effect of CH_3 defect in PE. However, we have not observed any noticeable difference in dielectric constant compared to perfect PE crystal, which may be due to the non-polar nature of CH_3 defect. Earlier simulation and experiment have proved that addition of polar side chain show higher increase in dielectric constant compared to non-polar side chain.^{25–28} Also, it has been noted that the introduction of large side chains causes larger increase in dielectric constant due to higher atomic relaxation in presence of electric field.

From the present study, it is clear that the addition of point-type polar chemical defect increases high-frequency dielectric constant. However, it does not provide additional atomic relaxation mechanism under electric field. Thus, the trend for $\Delta\epsilon$ remains very similar to perfect PE crystal. Addition of polar chemical species as defect shows same trend for high frequency. However, $\Delta\epsilon$ is highly anisotropic and depends critically on atomic relaxation mechanisms. Addition on small OH group increases static dielectric constant only in [001] direction due to small energy barrier for rotation. Addition of much bulkier COOH group increases static dielectric constant predominantly in [010] direction, where tilting of COOH group triggers realignment of its surrounding.

Our study suggests that it is possible to design a material with desired dielectric behavior by careful selection of defects in PE chain.

See [supplementary material](#) for method description, polarization calculations and movie S3.mov, S4.mov and S5.mov.

This work was supported by the Office of Naval Research through a Multi-University Research Initiative (MURI) grant N00014-17-1-2656. The computations were carried out at the Center for High Performance Computing of the University of Southern California.

REFERENCES

- ¹M. Ieda, *IEEE Trans. Electr. Insul.* **15**, 206 (1980).
- ²Q. M. Zhang, V. Bharti, and X. Zhao, *Science* **280**, 2101 (1998).
- ³H. B. Su, A. Strachan, and W. A. Goddard, *Phys. Rev. B* **70**, 64101 (2004).
- ⁴B. J. Chu, X. Zhou, K. L. Ren, B. Neese, M. R. Lin, Q. Wang, F. Bauer, and Q. M. Zhang, *Science* **313**, 334 (2006).
- ⁵V. Sharma, C. C. Wang, R. G. Lorenzini, R. Ma, Q. Zhu, D. W. Sinkovits, G. Pilianna, A. R. Oganov, S. Kumar, G. A. Sotzing, S. A. Boggs, and R. Ramprasad, *Nat. Commun.* **5**, 4845 (2014).
- ⁶S. Nasreen, G. M. Treich, M. L. Baczkowski, A. K. Mannodi-Kanakithodi, Y. Cao, R. Ramprasad, and G. Sotzing, *Kirk-Othmer Encycl. Chem. Technol.* **1** (2017).
- ⁷J. P. Jones, J. P. Llewellyn, and T. J. Lewis, *IEEE Trans. Dielectr. Electr. Insul.* **12**, 951 (2005).
- ⁸L. H. Chen, T. D. Huan, and R. Ramprasad, *Sci. Rep.* **7**, 6128 (2017).
- ⁹L. Chen, R. Batra, R. Ranganathan, G. Sotzing, Y. Cao, and R. Ramprasad, *Chem. Mater.* **30**, 7699 (2018).
- ¹⁰J. D. Hoffman, G. Williams, and E. Passaglia, *J. Polym. Sci. Part C Polym. Symp.* **14**, 173 (1966).
- ¹¹M. C. Righi, S. Scandolo, S. Serra, S. Iarlori, E. Tosatti, and G. Santoro, *Phys. Rev. Lett.* **87**, 76802 (2001).
- ¹²A. Moyassari, M. Unge, M. S. Hedenqvist, U. W. Gedde, and F. Nilsson, *J. Chem. Phys.* **146**, 204901 (2017).
- ¹³Y. Cao, P. C. Irwin, and K. Younsi, *IEEE Trans. Dielectr. Electr. Insul.* **11**, 797 (2004).
- ¹⁴P. Hohenberg and W. Kohn, *Phys. Rev.* **136**, B864 (1964).
- ¹⁵W. Kohn and L. J. Sham, *Phys. Rev.* **140**, A1133 (1965).
- ¹⁶T. Hakamata, K. Shimamura, F. Shimojo, R. K. Kalia, and A. Nakano, *Sci. Rep.* **5**, 19599 (2016).
- ¹⁷T. Onodera, K. Kawasaki, T. Nakakawaji, Y. Higuchi, N. Ozawa, K. Kurihara, and M. Kubo, *J. Phys. Chem. C* **118**, 11820 (2014).
- ¹⁸P. Umari and A. Pasquarello, *Phys. Rev. Lett.* **89**, 157602 (2002).
- ¹⁹P. Umari, *AIP Conf. Proc.* **677**, 269 (2003).
- ²⁰I. Souza, J. Íñiguez, and D. Vanderbilt, *Phys. Rev. Lett.* **89**, 117602 (2002).
- ²¹F. Shimojo, R. K. Kalia, A. Nakano, and P. Vashishta, *Phys. Rev. B* **77**, 1 (2008).
- ²²R. Resta, *Phys. Rev. Lett.* **82**, 4 (1998).
- ²³C. W. Bunn, *Trans. Faraday Soc.* **35**, 482 (1939).
- ²⁴Y. Huang, X. Wei, L. Liu, H. Yu, and J. Yang, *Mater. Lett.* **232**, 86 (2018).
- ²⁵S. Kraner, R. Scholz, C. Koerner, and K. Leo, *J. Phys. Chem. C* **119**, 22820 (2015).
- ²⁶S. Zhang, Z. Zhang, J. Liu, and L. Wang, *Adv. Funct. Mater.* **26**, 6107 (2016).
- ²⁷F. Jahani, S. Torabi, R. C. Chiechi, L. J. A. Koster, and J. C. Hummelen, *Chem. Commun.* **50**, 10645 (2014).
- ²⁸H. D. De Gier, F. Jahani, R. Broer, J. C. Hummelen, and R. W. A. Havenith, *J. Phys. Chem. A* **120**, 4664 (2016).